

***Ab initio* absorption spectra of  $Al_n$  ( $n=2-13$ ) clusters**

M. D. Deshpande\* and D. G. Kanhere†

*Department of Physics, University of Pune, Pune 411007, India*

Igor Vasiliev‡

*Department of Physics, New Mexico State University, Las Cruces, New Mexico 88003, USA*

Richard M. Martin§

*Department of Physics, University of Illinois at Urbana-Champaign, Urbana, Illinois 61801, USA*

(Received 12 August 2002; revised manuscript received 21 February 2003; published 30 July 2003)

We investigate the optical absorption spectra of  $Al_n$  ( $n=2-13$ ) clusters using the time-dependent spin-polarized local-density approximation. The overall shapes of the calculated spectra strongly depend on cluster geometries. It is observed that a simple jellium model is not valid for these clusters. In the size range of  $n \leq 5$ , the spectra show discrete, atomiclike transitions. For  $n=6-12$ , the shape of the absorption spectra can be explained on the basis of an ellipsoidal shell model. A strong collective excitation peak is observed for  $Al_{13}$  cluster, which is due to its spherical symmetry.

DOI: 10.1103/PhysRevB.68.035428

PACS number(s): 61.46.+w, 31.15.Ar

**I. INTRODUCTION**

The physics and chemistry of metal clusters continues to be a subject of intensive studies.<sup>1</sup> Clusters often possess unique properties different from both the extended bulk and the atomic states. Consequently, the study of the size evolution of various cluster properties, such as equilibrium geometries, stability, bonding nature, ionization potential, etc. is an interesting and challenging problem. In this context, the alkali-metal clusters, which are amenable to a jellium model interpretation, have been well studied.<sup>2</sup> The study of absorption spectra and the measurement of the average polarizability of clusters are very interesting since the polarizability and the shape of the spectra depend upon the cluster shape and size. The recent measurements of the total photoabsorption cross section of alkali-metal clusters<sup>3-6</sup> have been fitted to a collective resonance model which uses the principle values of the static polarizability tensor as fit parameters. The characteristics resonant peaks and their structure observed in the absorption spectra should therefore reflect the deviation of the true cluster geometry from a compact “spherical” shape.<sup>4,7</sup> In our earlier studies of mixed sodium-lithium clusters,<sup>8</sup> we observed that the topology varies with the composition, and the excited-state properties of such clusters get modified with the change in Li/Na content. All the calculated spectra demonstrate the presence of a strong plasmon peak. A closer examination of the oscillator strength led us to conclude that nonplasmon contributions are important for the case of  $Li_8$ .

Apart from the alkali-metal clusters, the aluminum clusters are among the most thoroughly investigated systems, both theoretically as well as experimentally.<sup>9</sup> Although the bulk aluminum is a free-electron metal, several experimental and theoretical studies indicate that small aluminum clusters do not display a well-known “magic” behavior.<sup>10,11</sup> Some experiments even suggest that the effective valency of Al atoms is 1 in small clusters.<sup>12</sup> Photoionization experiments are partially consistent with the shell model,<sup>13</sup> whereas non-

jellium behavior has been suggested from static dipole polarizability data.<sup>14</sup> In contrast to the alkali-metal clusters, two important issues concerning the Al clusters arise: the lack of  $s$  and  $p$  bands overlap and large perturbations due to +3 ionic core. These differences lead to serious deviations from the jellium model for aluminum clusters. The onset of the  $s$ - $p$  hybridization in pure Al clusters and the relation of their electronic structure to the jellium model has been studied by Duque and Mananes.<sup>15</sup> Photoelectron spectroscopy (PES) of the size selected anion<sup>16-18</sup> also provides information about the electronic and structural properties, as well as the  $s$ - $p$  hybridization of Al clusters.

These studies have led to the conclusion that the  $3s$ - $3p$  energy separation in Al clusters decreases with increasing the cluster size and that the  $s$  and  $p$  bands should begin to merge at a certain cluster size. It is expected that the jellium model is to work only in the range of sizes where the full  $s$ - $p$  mixing is achieved. Li *et al.*<sup>12</sup> have observed that the  $s$ - $p$  levels begin to overlap completely at  $n=9$ .

There are other critical issues concerning the nature of the electronic states in pure Al clusters: these have been critically examined by Rao and Jena.<sup>9</sup> They performed density-functional calculations for charged and neutral Al clusters and found that  $Al_7^+$  with 20 valence electrons is a magic cluster. Furthermore, they found that the electronic structures of clusters containing less than seven atoms do not correspond to the predictions based on a jellium model. They also presented some evidence for the monovalent nature of Al in small clusters. Similar studies of mixed  $Al_nX_m$  ( $X=Li, K$ ) clusters have failed to provide any evidence for suggested monovalent nature of Al.<sup>19,20</sup> Moreover, these studies showed that the alkalization of Al clusters makes the electronic structure to be jelliumlike. The alkalization also lowers the ionization potential of the base  $Al_n$  clusters.

All these observations have motivated us to calculate the absorption spectra of small  $Al_n$  ( $n=2-13$ ) clusters. We wish to extract the systematics from the spectra and to correlate it with the observations discussed above.

## II. COMPUTATIONAL DETAILS

The emphasis of the present work is on the systematics of the absorption spectra as function of cluster size in their ground state. As noted earlier, the ground state and other low-lying structures of Al clusters have been extensively studied by Rao and Jena.<sup>9</sup> Our ground-state geometries are identical to their geometries and were used as an input to calculate the polarizabilities and absorption spectra. Polarizabilities were calculated using a finite-field approach.<sup>21,22</sup> To do so, the Kohn-Sham equations were solved with and without a small electric field applied to the cluster of interest. The polarizability is defined by

$$\alpha_{ij} = \frac{\partial \mu_i(\mathbf{F})}{\partial F_j} = - \frac{\partial^2 E(\mathbf{F})}{\partial F_i \partial F_j}, \quad (1)$$

where  $i, j = \{x, y, z\}$  and the dipole moment is given by

$$\mu(\mathbf{F}) = \int \rho(\mathbf{r}) \mathbf{r} d\mathbf{r}. \quad (2)$$

In Eq. (1),  $E(\mathbf{F})$  is the total energy and  $F_i$  is the electric field applied along the  $i$ th axis. The average polarizability is calculated as the trace of the polarizability tensor,  $\alpha_{ij}$ ,

$$\langle \alpha \rangle = \frac{\alpha_{xx} + \alpha_{yy} + \alpha_{zz}}{3}. \quad (3)$$

The diagonal elements of the polarizability tensor can be obtained either from the dipole moment  $\mu(\mathbf{F})$  or from the total energy  $E(\mathbf{F})$  calculated at  $\mathbf{F}=0$  and  $\mathbf{F}=\pm \delta F_i$  using the standard finite-difference expressions for the first and second derivatives. Polarizability is known to be sensitive to the outer part of the electron density of a cluster. To ensure the proper convergence of the calculated polarizabilities, we increased the radius of the boundary sphere up to 22 a.u. and used a grid spacing of  $h=0.55$  a.u. The value of the applied electric field,  $\delta F$ , was chosen to be  $10^{-3}$  a.u. In all cases, polarizabilities calculated from the total energy and from the dipole moment coincided within 1%.

Absorption spectra were calculated using the time-dependent spin-polarized local-density approximation (TDLDA).<sup>23-26</sup> The system response is described by means of the coupling matrix, which can be used to calculate the true electronic excitations in the adiabatic approximation. The coupling matrix  $K_{ij\sigma,kl\tau}$  is given by

$$K_{ij\sigma,kl\tau} = \int \int \phi_{i\sigma}^*(\mathbf{r}) \phi_{j\sigma}(\mathbf{r}) \left( \frac{1}{|\mathbf{r}-\mathbf{r}'|} + \frac{\delta v_{\sigma}^{xc}(\mathbf{r})}{\delta \rho_{\tau}(\mathbf{r}')} \right) \times \phi_{k\tau}(\mathbf{r}') \phi_{l\tau}^*(\mathbf{r}') d^3 r d^3 r'. \quad (4)$$

The matrix indices  $i, j, \sigma$  in the above expression correspond to the occupied states, unoccupied states, and the spin index, respectively;  $\phi(\mathbf{r})$  are the Kohn-Sham one-electron wave functions, and  $v^{xc}(\mathbf{r})$  is the LDA exchange-correlation potential. The TDLDA electronic transition energies  $\Omega_n$  can be obtained from the solution of the eigenvalue problem:

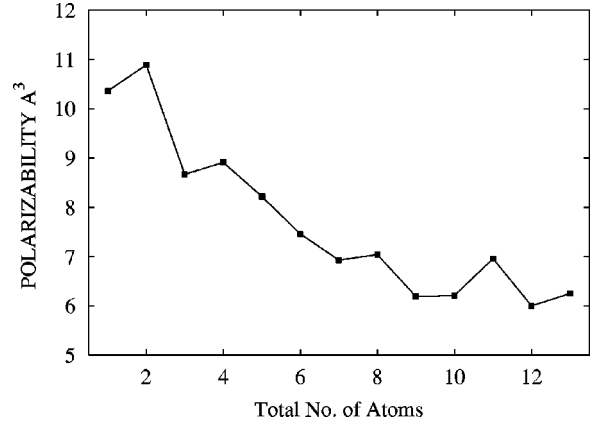


FIG. 1. Polarizabilities per atom for  $\text{Al}_n$  ( $n=1-13$ ) clusters shown vs the total number of atoms.

$$[\omega_{ij\sigma}^2 \delta_{ik} \delta_{jl} \delta_{\sigma\tau} + 2 \sqrt{f_{ij\sigma} \omega_{ij\sigma}} K_{ij\sigma,kl\tau} \sqrt{f_{kl\tau} \omega_{kl\tau}}] \mathbf{F}_n = \Omega_n^2 \mathbf{F}_n, \quad (5)$$

where  $\omega_{ij\sigma} = \epsilon_{j\sigma} - \epsilon_{i\sigma}$  are the Kohn-Sham transition energies, and the  $f_{ij\sigma} = n_{i\sigma} - n_{j\sigma}$  are the differences between the occupation of the  $i$ th and  $j$ th states, eigenvectors  $\mathbf{F}_n$  are related to the transition oscillator strengths.

These calculations were based on the Troullier-Martins nonlocal pseudopotentials<sup>27</sup> and Ceperley-Alder exchange-correlation functional.<sup>28</sup> To compute the absorption spectra, we used a spherical domain with a radius of 25 a.u., a grid spacing of 0.8 a.u. For all clusters, the number of unoccupied one-electron states included in the TDLDA calculations was taken to be at least three to five times greater than the number of occupied states. We have tested the convergence by taking the total number of states as 60, 80, 100.

## III. RESULTS AND DISCUSSION

First, we discuss the general features observed in these clusters. Small  $\text{Al}_n$  clusters ( $n \leq 5$ ) favor planar geometries. The lowest-energy structure for  $\text{Al}_3$  is an equilateral triangle while  $\text{Al}_4$  is rhombus with  $D_{2h}$  symmetry and is triplet. At  $n=6$ , structure changes from planar to a three-dimensional structure. For clusters containing from 11 to 13 atoms, an interior atom with the bulklike coordination emerges. The coordination number changes significantly at  $n=6$  and 11.

Figure 1 shows the average static polarizability (per atom) for  $\text{Al}_n$  clusters. We observe a similar trend in the case of measured polarizabilities of the atom and dimer.<sup>29</sup> The polarizability of the dimer is larger than the polarizability of the atom. In the case of alkalis, reverse is the case.<sup>30</sup> It is observed that aluminum cluster polarizabilities are at odds with jellium predictions for clusters up to 40 atoms. The ionization potential of aluminum clusters rises sharply for small  $n$ . We would expect that the rise of ionization potential connected to a more tightly bound molecules corresponds to a decrease of the polarizabilities per atom, as it does for alkalis. Small oscillations are superimposed on the average trend especially from  $n=7$  which is the onset of  $s$ - $p$  hybridization. From  $n=10$ , even-odd oscillations are observed.

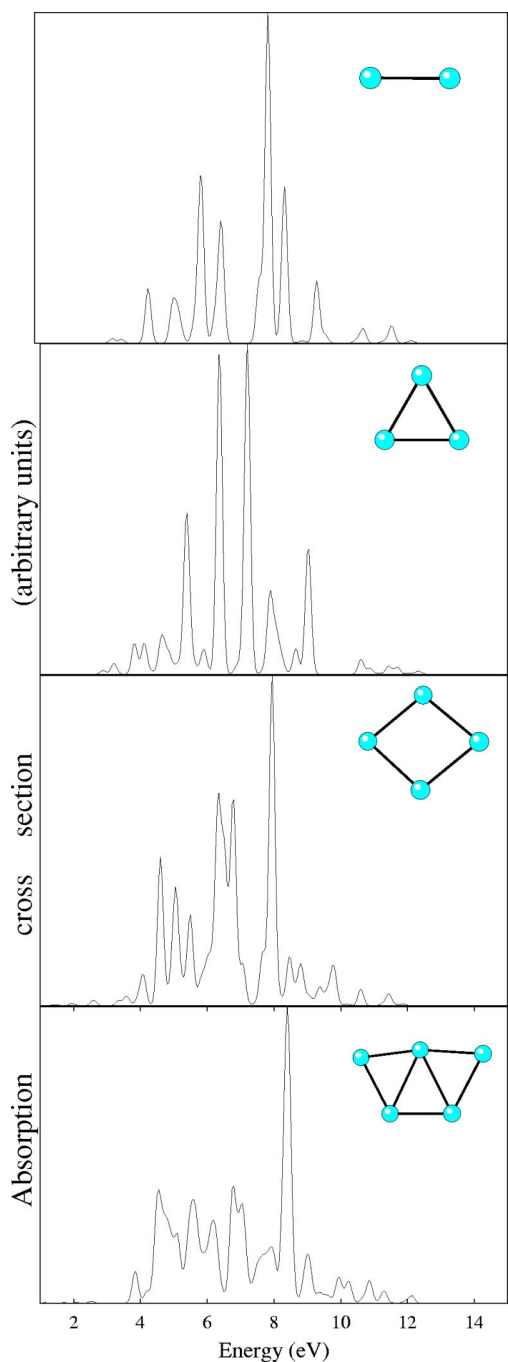


FIG. 2. The calculated TDLDA absorption spectra of  $Al_n$  ( $n = 2-5$ ) clusters. All TDLDA spectra are presented on the same relative scale. A Gaussian convolution of 0.1 eV has been used to simulate a finite broadening of the calculated spectra.

These characteristics are in agreement with the shell closing argument.

For the discussion of the absorption spectra, the geometries of  $Al_n$  clusters can be grouped according to the change in their coordination number as follows: (1)  $n = 2-5$ , (2)  $n = 6-10$ , (3)  $n = 11-13$ . The calculated absorption spectra along with the lowest-energy structures of neutral clusters are presented in Figs. 2-4.

Before discussing details of the systematics of the spectrum, we note some relevant observations emerging from

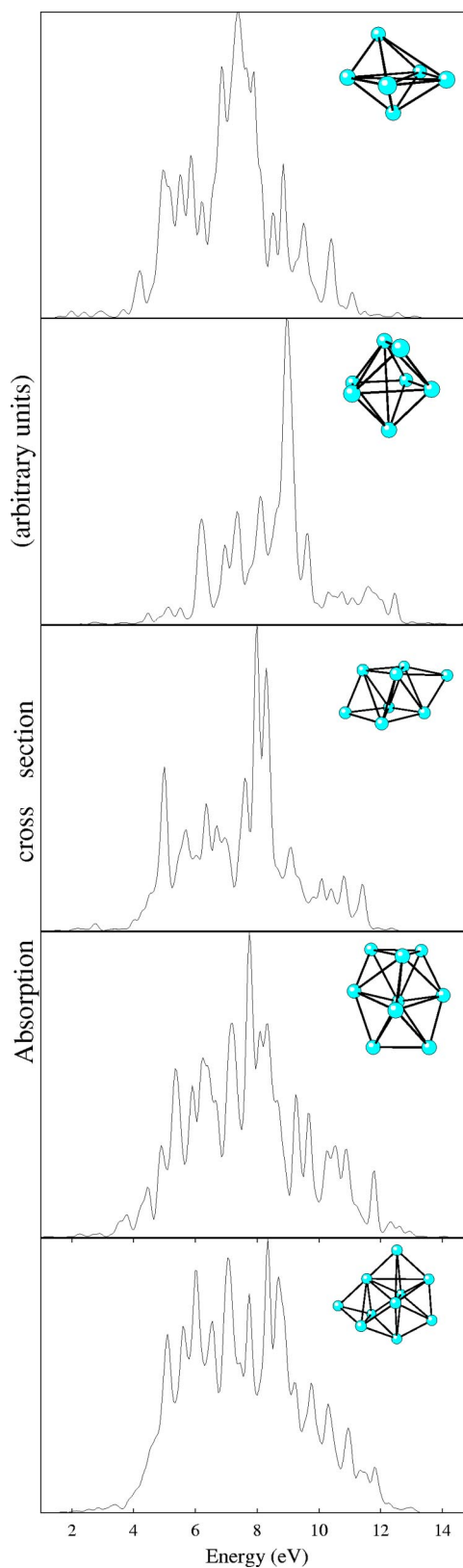


FIG. 3. The calculated TDLDA absorption spectra of  $Al_n$  ( $n = 6-10$ ) clusters.

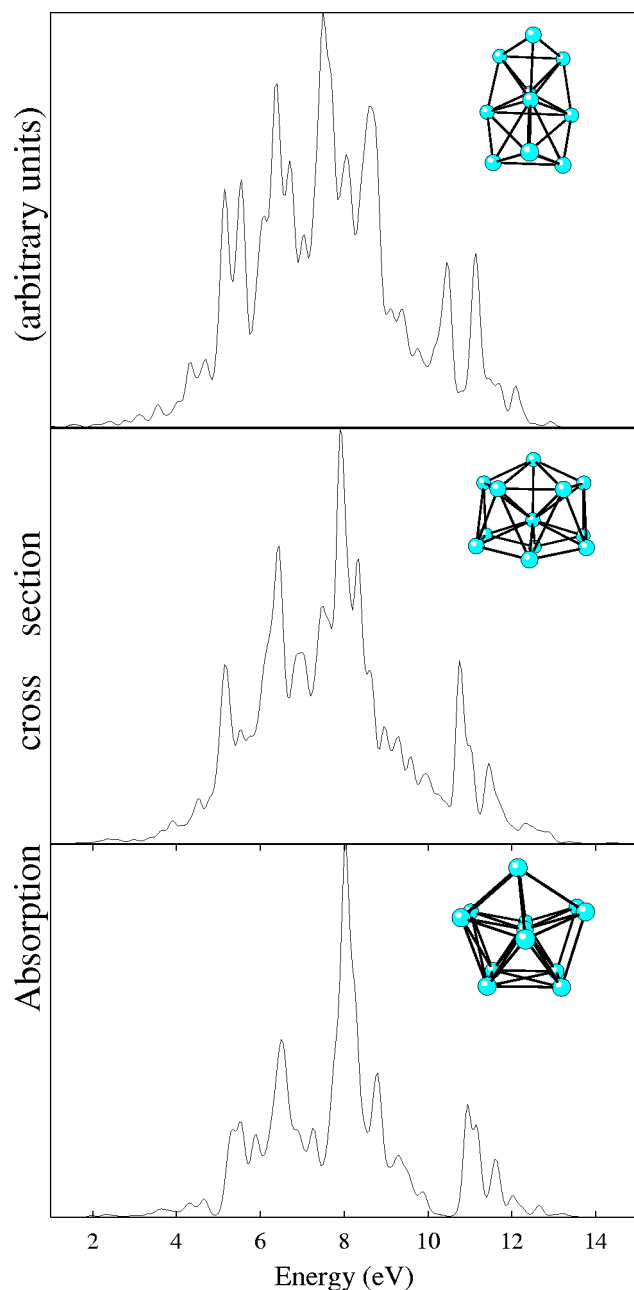


FIG. 4. The calculated TDLDA absorption spectra of  $Al_n$  ( $n=11-13$ ) clusters.

earlier studies.<sup>9</sup> The angular characteristics of the highest occupied molecular orbitals (HOMO) have been analyzed by Rao and Jena by using the linear combination of atomic orbitals method (LCAO). They have observed that for clusters with less than five atoms the HOMO is clearly an  $s$ -like orbital, while for the clusters containing more than seven atoms this orbital is clearly  $p$ -like. Clusters with  $5 \leq n \leq 7$  represent the region of transition.

It can be seen that for  $n \leq 5$ , the spectra of  $Al_n$  clusters are dominated by discrete, atomlike transitions. The dimer  $Al_2$  has been well studied and is known to have  $3\pi_u^2$  as a ground-state electronic configuration.<sup>31,32</sup> Among all dipole-allowed transitions, the most intensive transition occurs from the

lowest-valence state  $\sigma(s)$  to the lowest unoccupied molecular orbital (LUMO) of the cluster. The addition of the third atom changes the absorption spectrum significantly. The change could be attributed to a significant change in the geometry of the  $Al_3$  cluster.  $Al_3$  is an equilateral triangle with  $A_1^2$  symmetry. The increase in the number of absorption peaks indicates the discreteness of the level structure. The first dominant peak (nearer to 6 eV) occurs due to transition between  $2B^1$  state and LUMO's. The other dominant peak correspond to transitions between the LUMO,  $LUMO+k$  ( $k=8-11$ ) and to the doublet HOMO orbitals. The development of one additional peak is closely related to the involvement of the  $p$  orbital. A similar effect is also observed in the spectroscopic pattern for alkali-metal clusters.<sup>3,4</sup> According to a theory for nonspherical clusters,<sup>5</sup> the clusters immediately following a close-shell structure are usually distorted. This distortion reduces the energy of the newly populated level. It also reduces the oscillator strengths and the splitting of the absorption peaks, which reflects the breaking of the symmetry. The reduction of the oscillator strength and splitting of the absorption peaks are observed in  $Al_4$  and  $Al_5$  spectra.

For clusters with  $n \geq 6$ , the transition from discrete, atomlike excitations to quasicontinuous spectra is observed. The overall shapes of the absorption spectra in this size range can be discussed on the basis of an ellipsoidal shell model.<sup>5,6</sup> The change in the coordination number is accompanied by a breaking of electron degeneracies. At  $n=6$ , this change is related to the transition from the two-dimensional (2D) to three-dimensional (3D) geometries. The structural variation causes significant changes in the absorption spectrum of  $Al_6$  as compared to that of  $Al_5$ . The photoabsorption spectra are dominated by broad peaks, as expected for surface plasma resonance. Addition of one more Al atom to  $Al_6$  makes the structure more symmetric. The single peak in  $Al_7$  spectrum reflects the spherical symmetry of the cluster.  $Al_9$  is the smallest cluster that develops a pentagonal arrangement of atoms, which is a precursor to the icosahedral growth. As compare to  $Al_8$ , the number of high intensity peaks increases with the broadening of the spectra, which reflect a complete overlap of the  $s-p$  bands. According to an PES study, the  $s-p$  levels begin to overlap completely for  $n \geq 9$ .

The effects of shell closing are not observed significantly at  $n=11$ . Addition of one more atom makes the structure of  $Al_{12}$  more symmetric as compared to  $Al_{11}$ . As compared to the  $Al_{11}$  absorption spectrum, the number of high-intensity peaks get reduced.  $Al_{13}$  is a classic example for studying the relative stability of icosahedral and decahedron structures. The ground state of the 13-atom aluminum cluster is a Jahn-Teller distorted decahedron. The decahedral structure lies 0.25 eV/atom lower than the icosahedral structure. In the shell model of metal clusters,  $Al_{13}$  is nearly magic with 39 valence electrons. Negatively charged  $Al_{13}$  clusters are particularly abundant in mass spectrum. Due to the nearly spherical symmetry of the  $Al_{13}$  cluster, a single collective resonance is observed in the calculated spectrum. The spectrum profile of the icosahedron geometry (not shown) is nearly the same.

## IV. CONCLUSIONS

We have calculated the absorption spectra of the  $Al_n$  clusters in the size range of  $n=2-13$  using the time-dependent spin-polarized local-density approximation. The overall shapes and the structures of the calculated spectra strongly depend on cluster geometries. The simple jellium model is not valid for these clusters. In the size range of  $n \leq 5$ , the spectra of  $Al_n$  clusters are dominated by discrete, atomiclike transitions. For  $n=6-10$ , the shapes of the absorption spectra can be explained on the basis of an ellipsoidal shell model. At  $n=9$ , in the absorption spectra, we have observed complete overlap of the  $s$ - $p$  bands, which is consistent with

the PES study. For  $n=13$ , a strong, single collective excitation peak is observed in the optical spectrum due to the evolution of the spherical symmetry.

## ACKNOWLEDGMENTS

We gratefully acknowledge the Indo-French Center for the Promotion of Advanced Research (New Delhi)/Center Franco-Indian Pour la Promotion de la Recherche Avancee. M.D. acknowledges University Grants Commission, India for support. I.V. and R.M.M. acknowledge support for this work by the National Science Foundation for the Materials Computation Center at the University of Illinois.

\*Email address: mdd@physics.unipune.ernet.in

†Email address: kanhere@physics.unipune.ernet.in

‡Email address: vasiliev@nmsu.edu

§Email address: rmartin@uiuc.edu

<sup>1</sup>See, for example, *Physics and Chemistry of Finite Systems: From Clusters to Crystals*, edited by P. Jena, S. N. Khanna, and B. K. Rao (Kluwer Academic, Dordrecht, 1992).

<sup>2</sup>W.D. Knight, K. Clemenger, W.A. de Heer, W.A. Saunders, M.Y. Chou, and M.L. Cohen, *Phys. Rev. Lett.* **52**, 2141 (1984).

<sup>3</sup>W.D. Knight, K. Clemenger, W.A. de Heer, and W.A. Saunders, *Phys. Rev. B* **31**, 2539 (1985).

<sup>4</sup>K. Selby, V. Kresin, J. Masui, M. Vollmer, W.A. de Heer, A. Scheidemann, and W.D. Knight, *Phys. Rev. B* **43**, 4565 (1991).

<sup>5</sup>K. Clemenger, *Phys. Rev. B* **32**, 1359 (1985).

<sup>6</sup>K. Selby, M. Vollmer, J. Masui, V. Kresin, W.A. de Heer, and W.D. Knight, *Phys. Rev. B* **40**, 5417 (1989).

<sup>7</sup>C.R. Wang, S. Pollack, D. Cameron, and M.M. Kappes, *J. Chem. Phys.* **93**, 3787 (1990).

<sup>8</sup>M.D. Deshpande, D.G. Kanhere, P.V. Panat, I. Vasiliev, and R.M. Martin, *Phys. Rev. A* **65**, 053204 (2002).

<sup>9</sup>B.K. Rao, P. Jena, *J. Chem. Phys.* **111**, 1890 (1999), and references therein.

<sup>10</sup>B.K. Rao and P. Jena, *Phys. Rev. B* **32**, 2058 (1985).

<sup>11</sup>H. Hakkinen and M. Manninen, *Phys. Rev. Lett.* **76**, 1599 (1996).

<sup>12</sup>X. Li, H. Wu, X.B. Wang, and L.S. Wang, *Phys. Rev. B* **81**, 1909 (1998).

<sup>13</sup>K.E. Schriver, J.L. Persson, E.C. Honea, and R.L. Whetten, *Phys. Rev. Lett.* **64**, 2539 (1990); J.L. Persson and R.L. Whetten, *Chem. Phys. Lett.* **147**, 168 (1988).

<sup>14</sup>W.A. de Heer, P. Milani, and A. Chatelain, *Phys. Rev. Lett.* **63**, 2834 (1989).

<sup>15</sup>F. Duque and A. Mananes, *Eur. Phys. J. D* **9**, 223 (1999).

<sup>16</sup>J. Akola, M. Manninen, Hannu Hakkinen, U. Landman, Xi Li, and L. Wang, *Phys. Rev. B* **60**, R11 297 (1999).

<sup>17</sup>C. Chia-Yen, G. Gantefor, and W. Eberhardt, *J. Chem. Phys.* **100**, 995 (1994).

<sup>18</sup>H. Kawamata, Y. Negishi, A. Nakajima, and K. Kaya, *Chem. Phys. Lett.* **337**, 255 (2001).

<sup>19</sup>B.K. Rao and P. Jena, *J. Chem. Phys.* **113**, 1508 (2000).

<sup>20</sup>S. Chacko, M. Deshpande, and D.G. Kanhere, *Phys. Rev. B* **64**, 155409 (2001).

<sup>21</sup>H.A. Kurtz, J.J.P. Stewart, and K.M. Dieter, *J. Comput. Chem.* **11**, 82 (1990).

<sup>22</sup>A.A. Quong and M.R. Pederson, *Phys. Rev. B* **46**, 12 906 (1992); **46**, 13 584 (1992).

<sup>23</sup>M. E. Casida, in *Recent Advances in Density-Functional Methods*, edited by D. P. Chong (World Scientific, Singapore, 1995), Part I, p. 155; in *Recent Developments and Applications of Modern Density Functional Theory*, edited by J. M. Seminario (Elsevier Science, Amsterdam, 1996), p. 391.

<sup>24</sup>A. Rubio, J.A. Alonso, X. Blase, L.C. Balbas, and S.G. Louie, *Phys. Rev. Lett.* **77**, 247 (1996).

<sup>25</sup>J.M. Pacheco and J.L. Martins, *J. Chem. Phys.* **106**, 6039 (1997).

<sup>26</sup>I. Vasiliev, S. Ogut, and J.R. Chelikowsky, *Phys. Rev. Lett.* **82**, 1919 (1999), and references therein.

<sup>27</sup>N. Troullier and J.L. Martins, *Phys. Rev. B* **43**, 1993 (1991).

<sup>28</sup>D.M. Ceperley and B.J. Alder, *Phys. Rev. Lett.* **77**, 3865 (1996).

<sup>29</sup>P. Milani, I. Moullet, and W.A. de Heer, *Phys. Rev. A* **42**, 5150 (1990).

<sup>30</sup>D. Rayane, A.R. Allouche, E. Benichou, R. Antine, M. Aubert-Frecon, Ph. Dugourd, M. Broyer, C. Ristori, F. Chandezon, B.A. Huber, and C. Guet, *Eur. Phys. J. D* **9**, 243 (1999).

<sup>31</sup>R.O. Jones, *J. Chem. Phys.* **99**, 1194 (1993).

<sup>32</sup>K.K. Sunil and K.D. Jordon, *J. Phys. Chem.* **92**, 2774 (1988).